Optimization applied to dynamic poroelasticity using boundary element method (BEM) and genetic algorithm (GA)

Anunciação Jr.N. C, Anflor C.T.M, Goulart J.N.V

Research Article

Optimization applied to dynamic poroelasticity using boundary element method (BEM) and genetic algorithm (GA)

Anunciação Jr.N. C [*,1], Anflor C.T.M[1], Goulart J.N.V [1]

[1] *Group of Experimental and Computational Mechanics (GMEC), University of Brasilia, Brazil*

Article Info	Abstract
	This paper focused on developing a methodology based on coupling the Genetic Algorithm (GA) and the Boundary Element Method (BEM) for predicting the mechanical properties of a soil if a previous displacement x frequency curve is known. The NSGA-II (Elitist Non-Dominated Sorting Genetic Algorithm) was chosen for optimizing a dynamic poroelastic problem. The revisited problem introduced by Cheng is the benchmark used to verify the numerical routine and to apply the proposed optimization procedure. The present methodology was shown to be able to predict the mechanical properties of the underground soil if a displacement x frequency curve is previously known.

1. Introduction

During the last decade, countless efforts have been made to increase the capacity to exploit underground resources. It is well known that in the deepest regions there is a large amount of water, oil and gas reservoirs. The characteristics of the soil will determine what kind of resources will be present within it. The great complexity of the problems and the increasing availability of computational resources open up opportunities for the use of more comprehensive analyses. This kind of analysis is related to the concepts of soil mechanics that was first introduced by for Terzaghi [1] in the theory of elasticity and the theory of limit analysis (plasticity). Subsequently, Biot and Willis [2] presented the theory of consolidation, which is the basis for studies regarding to the poroelasticity of the soil.

The problems that arise in poroelasticity are related to the consolidation of layers of soil, excavations in saturated pores (such as tunnels), pumping (removal) of fluid (petroleum or water) by saturated porous medium, among others. The propagation of waves and consolidation of soil has long been a topic for study. Terzaghi [3] and Gassnann [4] provided wave propagation results in porous media at low frequency (0-100 Hz), considering the solid and fluid phases as unique. After some years analyzing the wave's propagation in poroelastic medium, Biot developed the theory of dynamic consolidation of soil. This study was divided in two parts, where the first one regards the elastic wave propagation in a saturated porous medium for low frequencies, and the second one for high frequencies. Through the previous studies introduced by Biot [5-6], two different types of wave propagation were observed, the primary and secondary. The primary is the compression or longitudinal waves and the secondary are the shear, distortion or

rotational waves. Plona [7] experimentally registered the existence of slow waves. In order to describe the porous medium two scales are needed. The first one is the macroscopic scale (related to the dimensions of a representative volume) and the second one is related to pore dimension which is microscopic in scale. These problems can be represented by using mathematical formulations, allowing the modelling through numerical methods. Introduced in this work is a numerical methodology for wave propagation based on Biot's theory of poroelasticity [8] coupled with Therzagi's theory of consolidation [1]. This numerical methodology applies the boundary element method (BEM) for solving the consolidation phenomena of poroelastic media problems. All differential equations were transformed into integral equations by using the reciprocity theorem. The behavior of poroelastic medium is still an object of study, and all the basic concepts solved by Biot can be applied. Schanz and Pryl [9] applied the poroelastic formulations in a dynamic analysis of compressible and incompressible media, i.e. solid and fluid. They observed that the behaviors of derivations of fundamental solutions confirmed the fact that the solid displacement and the pore pressure (fluid) are sufficient to describe the behavior of a poroelastic medium, affirming the theory of Biot. A simplified model of dynamic analysis on viscoelastic and poroelastic soils is presented by Millán and Domínguez [10], where dynamic coefficients of behavior were found through numerical formulations using the finite element method (FEM) and the BEM. Gensterblum [11] performed measurements of permeability in gases in the process of extraction of high quality bituminous coal, considering the dynamic and poroelastic aspects. The gases interaction and coupling of the gases were analyzed by using the Darcy's Equation. Hydraulic parameters were analyzed by Berg [12]. In this study the effects of pumping in aquifers resulted in pore pressure changes which were predicted by the traditional groundwater theory. Apostolakis and Dargush [13] used the analogy between thermoelastic and poroelastic theories first identified by Biot, and then developed a corresponding mixed variational principle for fluid-infiltrated porous bodies. They developed a poroelastic formulation in close mathematical analogy with the thermoelastic system particularized to the solid skeleton displacement, impulse of the effective stress, impulse of pore pressure and total average fluid displacement. According to this work, the physical analogy is not complete, as the contributions from the extended Fourier and Darcy laws are shown to be of a different character. In this sense, some efforts still need to be devoted to the development of new computational approaches in both problem domains (thermoelasticity and poroelasticity).

Considering this, the main goal of this work relies on applying an optimization process in such a way to predict the mechanical properties of soil if a frequency-displacement curve is known. A numerical routine was written in order to couple the NSGA-II (elitist non-dominated sorting genetic algorithm) and the BEM for evaluating a poroelastic dynamic problem. In this work, the Matlab GA toolbox was used while the BEM was completely written in open source code. The remainder of the paper is organized as follows. The poroelasticity theory and the basic equations for dynamic poroelasticity are the focus of Section 2. The development of the BEM for dynamic poroelasticity is presented in Section 3. Section 4 presents the GA methodology using NSGA-II as well as the objective function and the design variables. The theories introduced in the previous sections are applied for solving a revisited problem proposed by Cheng [14]. Finally, conclusions about the optimization process are provided in Section 5.

2. The Poroelasticity Theory

The internal structures of a porous body can be compared to a homogeneous solid, despite the presence of some voids between the grains. The voids can be completely filled or not by a fluid like water, gas or oil. In the theory of poroelasticity, the porous medium is considered as linear elastic, and the pores are considered competely filled with fluid. A

porous medium has a defined volume, which can be divided into two: the volume of the matrix and the volume corresponding to the pores. Porosity is defined by the ratio of pore volume to total volume. The effective stress introduced by Terzaghi [1, 15] is defined as that part that governs the deformation of the soil or rock. The effective stress can be decomposed into the sum of the effective stresses and the pore pressure as

$$\sigma_{ij} = \sigma'_{ij} + \alpha p \delta_{ij} \tag{1}$$

where σ_{ij} is the total stress, σ'_{ij} is the effective stress, p is the pore pressure (fluid pressure in the pores), δ_{ij} is the Kronecker delta and α is the Biot coefficient. For an isotropic media the stress can be written according to Eq. (2).

$$\sigma = \sigma' + \alpha p \tag{2}$$

2.1. Basic Equations for Dynamic Poroelasticity

According to Biot's theory (5), the equilibrium equations for linear poroelasticity are expressed as Eq. (3) and Eq. (4).

$$\tau_{ij,j} + X_i = \frac{\partial^2}{\partial t^2} \left(\rho_{11} u_i + \rho_{12} U_i \right) + k \frac{\partial}{\partial t} \left(u_i - U_i \right) \tag{3}$$

$$\tau_{,j} + X'_i = \frac{\partial^2}{\partial t^2} \left(\rho_{12} u_i + \rho_{22} U_i \right) + k \frac{\partial}{\partial t} \left(u_i - U_i \right) \tag{4}$$

where τ_{ij} is the solid stress, τ is the fluid stress due to the fluid pressure p introduced by Eq. (5).

$$\tau = -\beta p \tag{5}$$

where β is the porosity, u_i and U_i are the solid and fluid displacements, respectively. The variables ρ_{11}, ρ_{12} and ρ_{22} are the mass densities and X_i and X'_i concern the body force acting on the solid and fluid, respectively. The relations between the linear equilibrium equations and the mechanical variables are introduced by Eq. (6) and represents the partial solid stress and Eq. (7) the partial fluid stress.

$$\tau_{ij} = \left(\lambda + \frac{\alpha^2}{R} \right) \delta_{ij} e + 2\mu e_{ij} + \alpha \delta_{ij} \varepsilon \tag{6}$$

$$\tau = \alpha e + R \varepsilon \tag{7}$$

where δ_{ij} is the Kronecker delta, $e_{ij} = 0.5 \, (u_{i,j} + u_{j,i})$ is the solid strain tensor, $\varepsilon = U_{i,i}$ and $e = u_{i,i}$ are the fluid and solid dilation, respectively. Finally, there are the elastic constants λ, μ, α and R.

3. The Boundary Element Method for Dynamic Poroelasticity

The boundary integral formulation arises from the reciprocal relation between the terms of the displacements of the solid, boundary conditions of traction, stress in the fluid, boundary conditions of normal displacements in the fluid and body force in both phases. The integral representation for these equations can be written for 2D domain in the absence of body force according to Eq. (8) and (9), where J is defined as Eq. (10) according to Cheng [14].

$$c_{\alpha\beta} u_\alpha + \int_\Gamma t^*_{\alpha\beta} u_\alpha \, d\Gamma + \int_\Gamma \tau^*_\beta U_n \, d\Gamma = \int_\Gamma u^*_{\alpha\beta} t_\alpha \, d\Gamma + \int_\Gamma \tau U^*_{n\beta} \, d\Gamma \tag{8}$$

$$\int_\Gamma t^*_{\alpha 3} u_\alpha \, d\Gamma + \int_\Gamma \tau^*_3 U_n \, d\Gamma = \int_\Gamma u^*_{\alpha 3} t_\alpha \, d\Gamma + \int_\Gamma \tau \left(U^*_{n3} - J X'^*_\alpha n_\alpha \right) d\Gamma + J c_{33} \tau \tag{9}$$

$$J = \frac{1}{i\omega b - \omega^2 \rho_{12}} \tag{10}$$

The fundamental solutions for the solid and for the fluid are introduced by Eq. (11) and Eq. (12), respectively.

$$t^*_{\alpha j} = \left(\lambda e^*_j + \frac{\alpha}{R} \psi_{3j} \right) n_\alpha + 2\mu e^*_{\alpha j} \tag{11}$$

$$U^*_{nj} = J \left(\psi_{3j,\alpha} + \frac{1}{2\pi} \frac{r_{,\alpha}}{r} \delta_{3j} \right) n_\alpha + Z \, \psi_{\alpha j} \, n_\alpha \tag{12}$$

Where $Z = J(i\omega b + \omega^2 \rho_{12})$. The integrals are written as,

$$c^i u^i + \int_\Gamma p^* u \, d\Gamma = \int_\Gamma u^* p \, d\Gamma \tag{13}$$

Where u and p are vector fields from variables in Eq. (14) for solid displacement and fluid stress, respectively. The variables p^* and u^* are the fundamental solutions, as presented in Eq. (15).

$$u = \begin{bmatrix} u_1 \\ u_2 \\ \tau \end{bmatrix} \text{ and } p = \begin{bmatrix} t_1 \\ t_2 \\ U_n \end{bmatrix} \tag{14}$$

$$p^* = \begin{bmatrix} t^*_{11} & t^*_{21} & -U^*_{n1} \\ t^*_{12} & t^*_{22} & -U^*_{n2} \\ t^*_{13} & t^*_{23} & -\hat{U}^*_{n3} \end{bmatrix} \text{ and } u^* = \begin{bmatrix} u^*_{11} & u^*_{21} & -\tau^*_1 \\ u^*_{12} & u^*_{22} & -\tau^*_2 \\ u^*_{13} & u^*_{23} & -\tau^*_3 \end{bmatrix} \tag{15}$$

Where $\hat{U}^*n3 = U^*_{n3} - J X'^*_\alpha n_\alpha = (J \tau^*_{3,\alpha} + Zu^*_{\alpha 3})n_\alpha$ and c^i is introduced by Eq. (16).

$$c^i = \frac{1}{2} \begin{bmatrix} 1 & 0 & 0 \\ 0 & 1 & 0 \\ 0 & 0 & -J \end{bmatrix} \tag{16}$$

Considering the domain discretized in constant boundary elements Eq. (13) can be rewritten as,

$$c^i u^i + \sum_{j=1}^{N} \left\{ \int_{\Gamma_j} p^* \, d\Gamma \right\} u^j = \sum_{j=1}^{N} \left\{ \int_{\Gamma_j} u^* \, d\Gamma \right\} p^j \tag{17}$$

Eq. (17) can be also replaced according to Eq. (18) or Eq. (19).

$$c^i \, u^i + \sum_{j=1}^{N} \hat{H}^{ij} \, u^j = \sum_{j=1}^{N} G^{ij} \, p^j \tag{18}$$

$$\sum_{j=1}^{N} H^{ij} \, u^j = \sum_{j=1}^{N} G^{ij} \, p^j \tag{19}$$

One can also introduce Eq. (20) in order to take into account the coincidence between the source point and field point.

$$H^{ij} = \hat{H}^{ij} \qquad \text{when} \quad i \neq i$$
$$H^{ij} = \hat{H}^{ij} + c^i \qquad \text{when} \quad i = i \tag{20}$$

Equation (19) can be written as matrix,

$$H \, u = G \, p \tag{21}$$

where H and G are the influence coefficients matrices. For each node u_1 or t_1, u_2 or t_2 and τ or U_n are known variables and consequently $3N$ variables are unknown. Thus, the linear system as introduced in Eq. (20) can be rearranged, passing all unknown variables to the left side. This system can now be written as,

$$A \, X = F \tag{22}$$

where X is the unknown vector of displacement, traction, pore pressure and flux. F is a known vector and A is the coefficient matrix.

3. Genetic Algorithm

The genetic algorithm (GA) was originally proposed by John Holland [16] and it is based on the Darwinian principle of natural selection. The simplest genetic algorithm that still leads to good results in many practical problems is composed of four operators: selection, crossover, mutation and replacement. The selection operator is an artificial version of natural selection based on Darwinian survival of the fittest among string creatures. The crossover operator is performed after reproduction, creating two new populations from two existing ones by genetically recombining randomly chosen parts formed by a randomly chosen crossover point. The mutation is the operator that increases the possibility of finding the global optimum. This operator changes a percentage of individuals by altering the value of the existing string. The last operator is the replacement that is used to decide which individuals remain or are replaced in a population. There are many improvements on GA theory in order to make the optimization process more efficient and powerful. In this sense, many methodologies based on GA architecture have been developed. Based on some successful applications of optimization problems found in the literature, the NSGA-II was chosen as the GA algorithm. It is important to highlight that this algorithm uses a methodology where the concepts of dominance and diversity are applied simultaneously, which makes the NSGA-II an efficient tool in the search process and optimization of an objective function [15]. (Fig. 1) depicts a scheme of the NSGA-II structure used in this work.

The RMSE (root mean square error) was chosen as the objective function as introduced by Eq. (23). Minimizing the objective function, an approximation of the design variables results.

$$RMSE = \sqrt{\frac{\left(YY - Y\right)^2}{YY}} \tag{23}$$

where *YY* stands for the displacement obtained by numerical solution [12] and *Y* for the displacements obtained through an analytical solution.

The design variables that represent the poroelastic medium are stored in a vector *{E, G, ν, $ν_u$, B, α, R, k, ϕ}* = {Young's modulus, shear modulus, Poisson's coefficient, undrained Poisson's ratio, Skempton's pore pressure, Biot's coefficient, poroelastic constitutive coefficient, intrinsic permeability, porosity}, which will be maximized or minimized during the optimization process. Based on the specific sample of soils, the search space was defined according to Table 1.
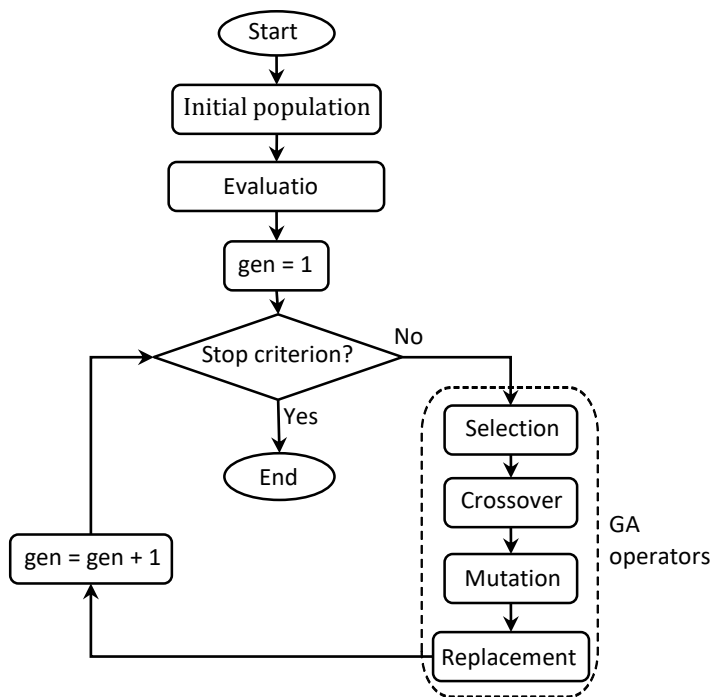

Fig. 1 GA scheme

Table 1 Search space

	Minimum	Maximum
G	1.5 x 1010	6 x 109
N	0.15	0.25
νu	0.31	0.34
B	0.50	0.85
K	4 x 10-4	8 x 102
ф	0.01	0.26

4. The Revisited Problem: Stress Excitation on Top of Column

A problem investigated by Cheng [14] is revisited in order to test the proposed methodology in this work. (Fig. 2) introduces a one-dimensional saturated soil or rock column with three possible excitation modes: a stress and pressure excitation at the top, and a displacement excitation at the bottom. Cheng [14] separately examined these excitations. Despite its importance, only the displacement excitation will be taken into account.
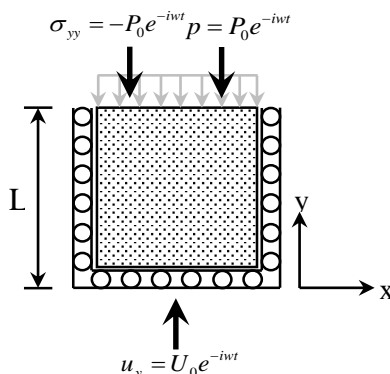

Fig. 2 One-Dimensional Saturated Soil Column under Dynamic Loading

It was considered that the top of the column was subject to a harmonic normal stress of $-P_0e^{-iwt}$ with the surface drained. The bottom and sides are confined by rigid, frictionless and impermeable walls. The imposed boundary conditions for this problem are introduced as,

$$\tilde{u}_y = 0 \; ; \; \tilde{q}_y = 0 \quad to \quad y = 0$$
$$\tilde{\sigma}_{yy} = -P_0 \; ; \; \tilde{p} = 0 \quad to \quad y = L$$

(24)

Cheng [14] and Dominguez [19] present the exact solution for the unidimensional poroelastic in terms of displacement, which can be obtained by using a mathematical symbolic computation program. They are presented as,

$$\frac{E_s \tilde{u}_y}{P_0 L} = \frac{d_3 \left[e^{-\lambda_1(L-y)} - e^{-\lambda_1(L+y)} \right]}{L(\lambda_3 d_1 - \lambda_1 d_3)(1 + e^{-2\lambda_1 L})} - \frac{d_1 \left[e^{-\lambda_3(L-y)} - e^{-\lambda_3(L+y)} \right]}{L(\lambda_3 d_1 - \lambda_1 d_3)(1 + e^{-2\lambda_3 L})}$$

(25)

$$E_s = \frac{2G(1-\nu)}{(1-2\nu)} \tag{26}$$

$$d_i = \frac{E_s \lambda_i^2 + \omega^2 (\rho - \beta\rho_f)}{\lambda_i (\alpha - \beta)} \tag{27}$$

$$\lambda_1 = \sqrt{\frac{-B_0 + \sqrt{B_0^2 - 4A_0C_0}}{2A_0}} \quad ; \quad \lambda_1 = \sqrt{\frac{-B_0 - \sqrt{B_0^2 - 4A_0C_0}}{2A_0}} \tag{28}$$

$$A_0 = \frac{E_s \beta}{\omega\rho_f} \; ; \; B_0 = \frac{\omega\beta(\rho - \beta\rho_f)}{\rho_f} + \frac{E_s \omega\phi^2}{R} + \omega(\alpha - \beta)^2 \text{ and}$$

$$C_0 = \frac{\omega^3 \phi^2 (\rho - \beta\rho_f)}{R} \tag{29}$$

Where E_s is the drained elastic property, ω is the frequency of excitation, ρ is the density of the soil (ρ_s stands for the solid density, ρ_f for the fluid density and ρ_a is the additional density) and λ_1 is the wave number and characterizes a high-velocity dilatational wave and λ_3 a low-velocity dilatational and dissipative wave [6]. For the routine calculations A_0, B_0 and C_0, it is necessary to calculate Biot's effective coefficient α, the constitutive coefficient poroelastic R and the force field β obtained through frequency depending on whether or not the material exhibits viscoelastic behavior [5]. The equation of the force field can be seen in Eq. (30).

$$\beta = \frac{\omega\phi^2 \rho_f k}{i\phi^2 + \omega k (\rho_a + \phi\rho_f)} \tag{30}$$

For this analysis, six material constants were used corresponding to the mechanical properties of Berea sandstone: G = 6.0 x 10^9 N/m², ν = 0.2; ν_u = 0.33; k = 1.9 x 10^{-10} m⁴/N.s; B = 0.62; ϕ = 0.19; ρ_s = 2800 kg/m³; ρ_f = 1000 kg/m³; ρ_a = 150 kg/m³ and a column length of L = 1 [16]. Dominguez [19] introduced a BEM formulation for dynamic poroelastic problems. The efforts were initially devoted to the analysis of the Biot coefficients and the development of the boundary integral equations in terms of solid displacement and fluid stress. Selvadurai [20] also introduced an analysis about waves for poroelastic media, applying the statements proposed by Cheng [14] and Dominguez [19]. In order to validate the methodology introduced by Domingues [19] and apply the proposed formulation by Biot [8], the vertical displacements obtained by the excitation at the top of a column were calculated. The numerical solutions were analyzed and compared with the analytical solution introduced by Cheng [14], using the same constant materials previously defined by Rice and Cleary [18]. This same analysis was performed using the principles of the Biot theory by Selvadurai [20] using the BEM for studying wave propagation in a saturated poroelastic media. In this study, peaks of resonance for low frequencies $\omega_n = (2n-1)\omega_1$, were found, with n = 1,2,3, ... (Fig. 2) depicting the numerical solution versus the analytical solution. The results were plotted in absolute values of normalized displacement at the top of the column $\tilde{u}_y(L)E_u/P_0L$ versus the dimensionless frequency $\omega^* = \omega/\omega_1$. The first frequency of resonance ω_1 can also be determined by Eq. (40) and E_u is the undrained elastic module as introduced by Eq. (41). According to Selvadurai [20], for frequencies below the first natural frequency, the dimensionless displacement approximates the values of the poroelastic displacements for the elastic behavior.

$$\omega_1 = \frac{\pi}{2L}\sqrt{\frac{E_u}{\rho}} \tag{40}$$

$$E_u = \frac{2G(1-\nu_u)}{(1-2\nu_u)} \tag{41}$$

The problem initially introduced by Selvadurai [20] followed by Dominguez [19] was discretized into 24 constant elements, numerically integrated with four Gauss points and considers a discrete set of 44 frequencies. (Fig. 3) depicts the perfect overlapping until $\omega = 2.5\,\omega_1$ where after this point, it is possible to see a small offset between both curves.
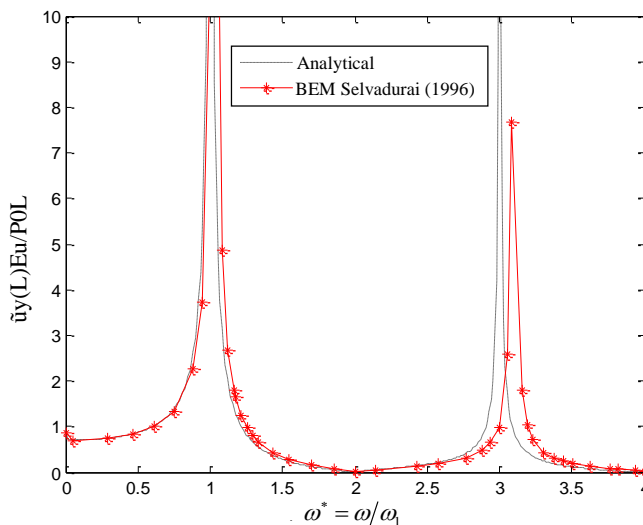

Fig. 3 Displacement at the top of the column (stress excitation)

5. The Numerical Results Using GA And BEM

In order to define the mechanical properties of the soil, a numerical routine was written to couple both, the GA and the BEM. The domain was discretized into 32 constant boundary elements and integrated numerically with six Gauss points. A set of 327 frequencies was defined in order to ensure a good definition of the curves and the resonance peaks. The objective function as aforementioned, was the RMSE and the design variables to be optimized were: G, ν, ν_u, B, k, and ϕ. Table 2 summarizes the maximum and minimum values for the search space, the values of the material constant imposed for the analytical solution and those obtained after the optimization process. According to the resulting mechanical properties after the optimization process, it is suggested that the soil is Berea sandstone.

The numerical results are related to the permeability of the soil in consequence of the fluid trapped in the pores and the volumetric reaction of the process with fluid and solid. The deformations present elastic behavior and are linked as variables of the optimization process. The numerical results are related to the frequencies (ω) of the loads.

After searching fields in approximately 10 thousand iterations in the GA, the three variables that most influenced the process were: permeability (k) because it is related to a

quantity of pores (ϕ) and the interconnection between them affecting soil poropressure behavior; the shear coefficient (G) that can approach a maximum stress, allowing a quantity of material (ideal); and the Poisson coefficient drained (v_u) being the most differentiated coefficient. Since there is load dynamics in the structure, it was made with this parameter to undergo great influence without calculation.

Table 2 Design variables, search range, analytical and optimized variables.

Design variables	Search space max	Search space min	Analytical	Optimized
G	6 x 109	6 x 1019	6 x 109	5.95 x 109
N	0.20	0.18	0.20	0.20
vu	0.33	0.28	0.33	0.31
B	0.62	0.50	0.62	0.61428
K	1.9 x 102	5.6 x 100	1.9 x 102	9.54 x 10-1
φ	0.19	0.19	0.19	0.195

The stop criterion was set to approximate the values of the variables through the optimization process with a minimum possible value; therefore, it was used as the reference in Eq. (23) in RMSE ≤ 0.025 and was achieved for a value of 0.02509069.

A comparison between the analytical curve and the optimized one, can be seen as (Fig. 3) (load transmitted by dynamic pressure) with the effects of the distribution of the AG coupled to the BEM overlapping the analytic curve adopted by Cheng [14].

It is possible to observe a proximity between the solutions, and as in Selvadurai [20] there was no total overlap of the curves. Full overlap requires a thorough investigation of the problem.
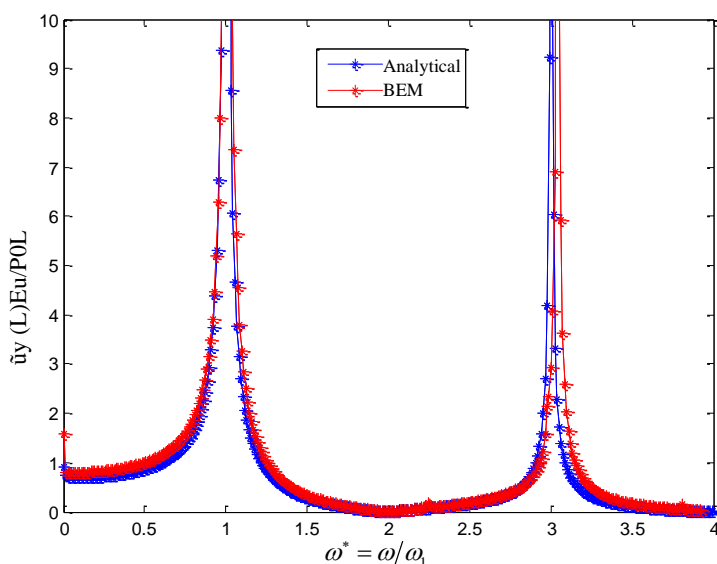

Fig. 3 Displacement at the top of the column (stress excitation)

5. Conclusions

The main goal of this work was to develop a numerical procedure using BEM and GA-NSGA-II in order to determine the design variables G, B, k, v, v_u, and ϕ as mechanical properties of soil. The presented methodology was shown to be efficient for predicting the kind of underground soil if a displacement x frequency curve is previously known. Despite using an analytical curve for the displacement x frequency behavior, the present methodology can also be used with a curve obtained experimentally. Regarding the design variables, it is important to highlight that the permeability (k) was the variable that was most influenced during the optimization process. The main reason is due to the fact that this variable takes into account the amount of pores, the connection between them and finally the strong influence in the fluid percolation. All advantages from the BEM features provided a low computational cost and resulted in a good prediction for the characterization of the soil.

References

[1] Terzaghi, K. (1925). "Principles of soil mechanics, IV—Settlement and consolidation of clay". Engineering News-Record, 95(3), 874-878.

[2] Biot, M. A. and Willis, D. G. (1956). "The elastic coefficients of the theory of consolidation". J. Appl. Mech., 24, 594-601.

[3] Terzaghi, K. (1936). "The shearing resistance of saturated soils and the angle between the planes of shear". Proceedings of the International Conference on Soil Mechanics and Foundation Engineering, pp. 54-56.

[4] Gassmann, F. (1951). "Elasticity of porous media". Vierteljahrsschrder Naturforschenden Gesselschaft, 96, 1-23.

[5] Biot, M. A. (1956a). "Theory of propagation of elastic waves in a fluid-saturated porous solid. I. Low- frequency range". Journal of Applied Physics. Nr 28. pp. 168-178. https://doi.org/10.1121/1.1908239

[6] Biot, M. A. (1956b). "Theory of propagation of elastic waves in a fluid-saturated porous solid. I. High- frequency range". Journal of Applied Physics. Nr 28. pp. 179-191.

[7] Plona, T. J. (1980). "Observation of a second bulk compressional wave in a porous medium at ultrasonic frequencies". Appl. Phys. Lett., 36:259-261. https://doi.org/10.1063/1.91445

[8] Biot, M. A. (1956). "Theory of Deformation of a Porous Viscoelastic Anisotropic Solid", Journal of Applied Physics, vol. 27, pp 459 - 467. https://doi.org/10.1063/1.1722402

[9] Schanz, M., Pryl, D. (2004). "Dynamic fundamental solutions for compressible and incompressible modeled poroelastic continua". International Journal of Solids and Structures, 41(15), 4047-4073. https://doi.org/10.1016/j.ijsolstr.2004.02.059

[10] Millán, M. A., & Domínguez, J. (2009). "Simplified BEM/FEM model for dynamic analysis of structures on piles and pile groups in viscoelastic and poroelastic soils". Engineering Analysis with Boundary Elements, 33(1), 25-34. https://doi.org/10.1016/j.enganabound.2008.04.003

[11] Gensterblum, Y., Ghanizadeh, A., and Krooss, B. M. (2014). "Gas permeability measurements on Australian subbituminous coals: fluid dynamic and poroelastic aspects". Journal of Natural Gas Science and Engineering, 19, 202-214. https://doi.org/10.1016/j.jngse.2014.04.016

[12] Berg, S. J., Hsieh, P. A., and Illman, W. A. (2011). "Estimating hydraulic parameters when poroelastic effects are significant". Groundwater, 49(6), 815-829. https://doi.org/10.1111/j.1745-6584.2010.00781.x

[13] Apostolakis, G., & Dargush, G. F. (2013). "Mixed variational principles for dynamic response of thermoelastic and poroelastic continua". International Journal of Solids and Structures, 50(5), 642-650. https://doi.org/10.1016/j.ijsolstr.2012.10.021

[14] Cheng, A. H. D., Badmus, T., Beskos, D. E. (1991). "Integral equation for dynamic poroelasticity in frequency domain with BEM solution". Journal of Engineering Mechanics, 117(5), 1136-1157. https://doi.org/10.1061/(ASCE)0733-9399(1991)117:5(1136)

[15] Terzaghi, K. (1923). "Die Berechnung der Durchlässigkeitsziffer des Tones aus dem Verlauf der hydrodynamische Spannungserscheinungen". Sitzber. Akad. Wiss. Wien, Abt. IIa, 132, 125-138.

[16] Holland, J. H. (1975). "Adaptation in Natural and Artificial Systems. University of Michigan Press". Ann Arbor.

[17] Deb, K.; Agrawal, S.; Pratab, A.; Meyarivan, T. (2000). "A fast elitist non-dominated sorting genetic algorithm for multi-objective optimization: NSGA-II". Kangal Report 200001, Indian Institute of Technology, Kanpur, India. https://doi.org/10.1007/3-540-45356-3_83

[18] Rice, J. R., Cleary, M. P. (1976). "Some basic stress diffusion solutions for fluid-saturated elastic porous media with compressible constituents." Reviews of Geophysics and Space Physics, V.14, N.2, P.227-41. https://doi.org/10.1029/RG014i002p00227

[19] Dominguez, J. (1993). "Boundary elements in dynamics". Wit Press.

[20] Selvadurai, A. P. S. (1996). Mechanics of poroelastic media. In Antes, H., & Wiebe, T. "Analyses of waves in 3-d poroelastic media". (Pp. 371-387). Springer Netherlands. https://doi.org/10.1007/978-94-015-8698-6